# The Talpid3 gene (KIAA0586) encodes a centrosomal protein that is essential for primary cilia formation

Development 136, 655-664 (2009) doi:10.1242/dev.028464

# The *Talpid3* gene (*KIAA0586*) encodes a centrosomal protein that is essential for primary cilia formation

**Yili Yin[1,*], Fiona Bangs[2,*], I. Robert Paton[3], Alan Prescott[4], John James[4], Megan G. Davey[3], Paul Whitley[2], Grigory Genikhovich[5], Ulrich Technau[5], David W. Burt[3] and Cheryll Tickle[2,†]**

The chicken *talpid*$^3$ mutant, with polydactyly and defects in other embryonic regions that depend on hedgehog (Hh) signalling (e.g. the neural tube), has a mutation in *KIAA0568*. Similar phenotypes are seen in mice and in human syndromes with mutations in genes that encode centrosomal or intraflagella transport proteins. Such mutations lead to defects in primary cilia, sites where Hh signalling occurs. Here, we show that cells of *talpid*$^3$ mutant embryos lack primary cilia and that primary cilia can be rescued with constructs encoding Talpid3. *talpid*$^3$ mutant embryos also develop polycystic kidneys, consistent with widespread failure of ciliogenesis. Ultrastructural studies of *talpid*$^3$ mutant neural tube show that basal bodies mature but fail to dock with the apical cell membrane, are misorientated and almost completely lack ciliary axonemes. We also detected marked changes in actin organisation in *talpid*$^3$ mutant cells, which may explain misorientation of basal bodies. KIAA0586 was identified in the human centrosomal proteome and, using an antibody against chicken Talpid3, we detected Talpid3 in the centrosome of wild-type chicken cells but not in mutant cells. Cloning and bioinformatic analysis of the Talpid3 homolog from the sea anemone *Nematostella vectensis* identified a highly conserved region in the Talpid3 protein, including a predicted coiled-coil domain. We show that this region is required to rescue primary cilia formation and neural tube patterning in *talpid*$^3$ mutant embryos, and is sufficient for centrosomal localisation. Thus, Talpid3 is one of a growing number of centrosomal proteins that affect both ciliogenesis and Hh signalling.

**KEY WORDS: Primary cilia, Centrosome, Hedgehog signalling, Ciliopathies, Talpid3, Chicken, Neural tube, Embryo**

## INTRODUCTION

The chicken *talpid*$^3$ mutant has a complex phenotype, including polydactylous limbs with many unpatterned digits, vascular defects, hypoteleorism, abnormal dorsoventral patterning of the neural tube, loss of endochondral bone formation and embryonic lethality (Davey et al., 2007; Davey et al., 2006; Ede and Kelly, 1964a; Ede and Kelly, 1964b). Development of all the regions affected in the *talpid*$^3$ mutant embryo requires Hedgehog (Hh) signalling and analysis of the developing mutant limb bud and neural tube has shown that it is the response to Hh signalling that is defective (Lewis et al., 1999). Expression of some downstream Shh target genes in *talpid*$^3$ mutant limb buds, head, neural tube and somites is lost, whereas other genes are expressed more widely, suggesting that there is failure both to activate gene expression in response to Shh and to repress gene expression in its absence (Buxton et al., 2004; Davey et al., 2006; Lewis et al., 1999). These opposing effects can be understood in terms of the bifunctionality of the Gli proteins, the transcriptional effectors of vertebrate Hedgehog (Hh) signalling, which function as activators (mainly Gli1, Gli2) or are processed to short forms (mainly Gli3) that function as repressors (Aza-Blanc et al., 2000; Bai et al., 2002; Marigo et al., 1996; Ruiz i Altaba, 1999). Indeed, direct analysis of Gli3 proteins in *talpid*$^3$ mutant tissues showed that Gli3 processing is abnormal, although translocation to the nucleus still occurs (Davey et al., 2006). We have identified *KIAA0586* (*Talpid3*) as the gene affected in *talpid*$^3$ mutant embryos (Davey et al., 2006). *KIAA0586* is ubiquitously expressed and encodes a novel protein with no previously known function (Davey et al., 2006).

The phenotype of *talpid*$^3$ mutant chicken embryos, including the inability to process Gli3, is strikingly similar to that of mouse embryos with mutations in genes encoding centrosomal or intraflagellar transport (IFT) proteins, such as *Arl13b*, *OFD1*, *Polaris*, *IFT172*, *Kif3a*, *Dnchc2* and *Ftm* (Caspary et al., 2007; Ferrante et al., 2006; Haycraft et al., 2005; Huangfu et al., 2003; May et al., 2005; Vierkotten et al., 2007). These mouse mutants lack normal primary cilia, the site where cells receive Shh signals and other cell-cell signals (Corbit et al., 2005; Eggenschwiler and Anderson, 2007; Rohatgi et al., 2007). An increasing number of human syndromes, collectively known as ciliopathies, which affect cilia formation and function, also have phenotypic features similar to *talpid*$^3$ mutant chickens, such as polydactyly (Badano et al., 2006; Bisgrove and Yost, 2006; Eley et al., 2005; Fliegauf et al., 2007; Pazour and Rosenbaum, 2002; Tobin and Beales, 2007). Interestingly, *KIAA0586* was identified in a human centrosome proteome (Andersen et al., 2003). We have therefore investigated whether the mechanism underlying abnormal Hh signalling in the *talpid*$^3$ mutant involves a failure of primary cilia formation and whether the Talpid3 protein is enriched in the ciliary apparatus.

## MATERIALS AND METHODS

### Embryos

Fertilised White Leghorn chicken eggs were obtained from H. Stewart (Lincolnshire) and incubated at 37°C and staged according to Hamburger and Hamilton (Hamburger and Hamilton, 1992). *Talpid*$^3$ carriers were maintained as described previously (Davey et al., 2006).

[1]Division of Cell and Developmental Biology, Wellcome Trust Biocentre, The University of Dundee, Dundee DD1 5EH, UK. [2]Department of Biology and Biochemistry, University of Bath, Bath BA2 7AY, UK. [3]Department of Genetics and Genomics, The Roslin Institute and Royal (Dick) School of Veterinary Studies, The University of Edinburgh, Midlothian EH25 9PS, UK. [4]Centre for High Resolution Imaging and Processing, The University of Dundee, Dundee DD1 5EH, UK. [5]Developmental Biology Section, Faculty for Life Sciences, University of Vienna, Althanstrasse 14, 1090 Wien, Austria.

*These authors contributed equally to this work
†Author for correspondence (e-mail: cat24@bath.ac.uk)

**Accepted 11 December 2008**

### Section immunohistochemistry

Embryos were fixed in 4% PFA for 2 hours at room temperature (RT) and genotyped as described previously (Davey et al., 2006). Selected embryos embedded in 10% sucrose, 7.5% gelatine were sectioned at 10 μm or 40 μm. Sections were stained as described previously (Das et al., 2006). Primary antibodies were as follows: for visualisation of primary cilia, rabbit anti-γ-tubulin 1:1000 (Sigma) and mouse anti-acetylated tubulin 1:1000 (Sigma); for microtubules, mouse anti α-tubulin 1:1000 (Sigma); mouse anti-Islet1 1:10 (Developmental Studies Hybridoma Bank; DSHB), mouse anti-NKX2.2 1:5 (DSHB), mouse anti-PAX6 1:2 (DSHB), mouse anti-PAX7 1:10 (DSHB); and for filamentous actin, Alexa Fluor 546 phalloidin 1:100 (Molecular Probes). Secondary antibodies were: Alexa-Fluor-488 conjugated anti-mouse 1:500 (Molecular Probes), Alexa-Fluor-546 conjugated anti-rabbit 1:500 (Molecular Probes) and Alexa-Fluor-610 conjugated anti-rabbit 1:1000 (Molecular Probes). Sections counterstained with DAPI, viewed using Leica DMR compound microscope or Zeiss LSM510 or Nikon eC1 laser scanning confocal microscope.

### Electronmicroscopy

Stage HH24 chicken embryos treated as described previously (Davey et al., 2007). For SEM, samples washed in 100% acetone for 10 minutes before critical point drying, flushed five times to ensure excess acetone was removed, dried, then placed on carbon mounts, coated with Au/Pd and imaged using an ESEM at 15 kV, 10 mm WD in high vacuum mode. For TEM sections cut between 70-100 nm and viewed with FEI Tecnai 12 transmission electron microscope.

### Histology

Seven-day-old embryos fixed 4% PFA overnight, washed in PBS, dehydrated into 100% xylene, then wax embedded overnight. Sections were cut at 5 μm, dewaxed, stained with Hematoxylin and Eosin, and photographed using Leica DMR compound microscope.

### Neural tube electroporation

The lumen of the neural tube of stage HH10-14 *talpid*$^3$ mutant flock embryos was injected with 1 μg/μl of construct encoding either full-length chicken Talpid3 (ggKIAA0586) or fragments of chicken Talpid3 in pCAGGs, plus 0.1 μg/μl pCAGGS-RFP and 0.02% Fast Green, and electroporated with square wave current of 25 mV applied five times for 15 mseconds (CUY21 electroporator, Protech International, TX, USA). Embryos were incubated for a further 48 hours, which is when mutant embryos can be identified, then fixed and sectioned.

### Cell culture for examination of cilia formation, cilia rescue and cytoskeletal organisation

Chick embryonic fibroblasts (CEFs) were generated from HH24 embryo bodies by cutting the tissue into small pieces before trypsinising for 1-2 minutes. Trypsin was inhibited with serum, tissue disaggregated, cells spun down and then resuspended in fresh DMEM/Ham's F12 (Gibco) plus 10% foetal calf serum (FCS). Cells were passaged twice before use. Primary cell cultures were generated from HH24 limb buds, by trypsinisation for 1-2 minutes, tissue disaggregated, then cells spun down and resuspended in 20 μl of DMEM and seeded onto fibronectin (SIGMA) coated 13 mm coverslips. Cells were left to adhere for 1 hour before flooding with DMEM/Ham's F12+10% FCS. HEK293T cells were maintained in DMEM+10% FCS under normal cell culture conditions.

In test for rescue of primary cilia, CEFs were seeded onto coated 13 mm coverslips at $1\times10^6$/ml and transfected with a construct encoding full-length chicken Talpid3 in pCAGGS (ggKIAA0586) using Fugene6 (Roche) for 48 hours. When near confluence, cells were synchronised in serum-free medium for 2 days, then fixed and stained.

For localisation of tagged Talpid3, HEK293T cells were seeded onto 13 mm coverslips at $1\times10^6$/ml, then grown for 18-24 hours before transfection with 1 μg ggKIAA0586::Myc or Flag::ggKIAA0586. For localisation of GFP fusion construct, primary chicken cell cultures or HEK293T

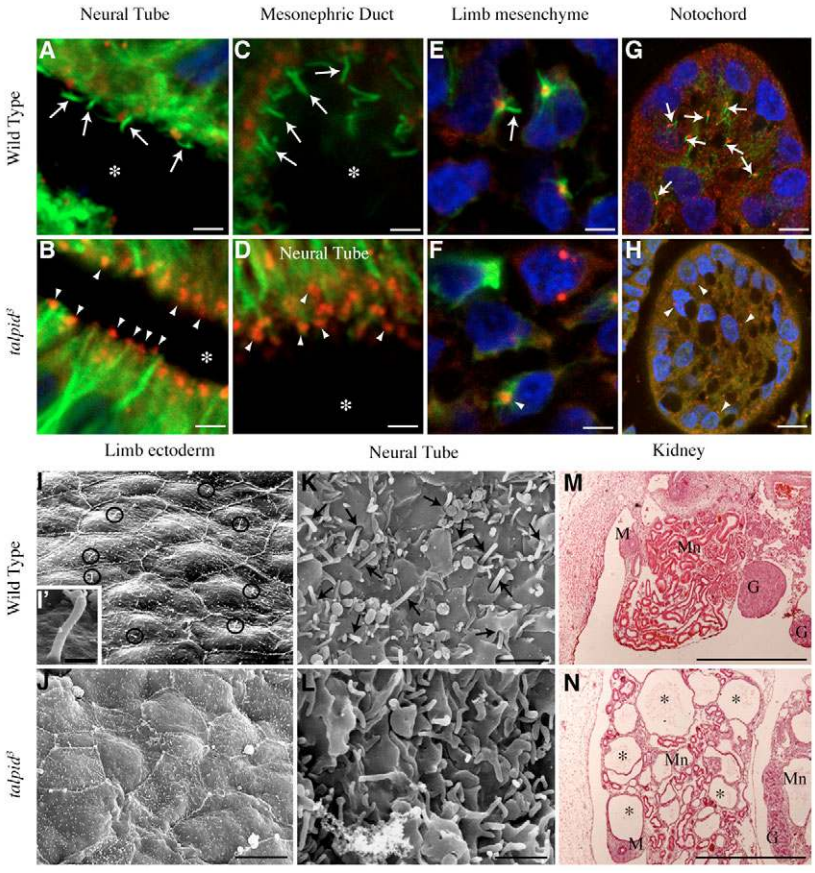


**Fig. 1. Primary cilia defect in *talpid*$^3$ mutant embryos.** Immunostaining of sections of wild type (A,C,E,G) and *talpid*$^3$ mutant (B,D,F,H) chicken embryos; anti-γ tubulin (red) for centrosome; anti-acetylated tubulin (green) for ciliary axoneme. (**A**) Wild-type neural tube, primary cilia (arrows) protruding into lumen (*) from centrosomes. (**B**,**D**) *talpid*$^3$ mutant neural tube (centrosomes are indicated with arrowheads), ciliary axonemes absent, compare with A. (**C**) Wild-type mesonephric duct; primary cilia (arrows) protruding from centrosomes into lumen (*). (**E**) Wild-type limb bud; primary cilia on mesenchyme cells (arrow). (**F**) *talpid*$^3$ mutant limb bud; centrosomes are indicated with an arrowhead on mesenchyme cells, cilia axonemes are absent (compare with E). (**G**) Wild-type notochord; primary cilia project from centrosomes (arrows). (**H**) *talpid*$^3$ mutant notochord; centrosomes are indicated with arrowheads, ciliary axonemes are absent, compare with G. (**I-L**) SEM of dorsal surface of wing bud and luminal surface of neural tube from HH24 embryos. (I) Wild-type wing bud; black circles indicate primary cilia. (I') A higher magnification of primary cilium. (J) *talpid*$^3$ mutant wing bud; no primary cilia visible. (K) Wild-type neural tube; black arrows indicate primary cilia emerging from pits on apical surface of cells lining lumen. (L) *talpid*$^3$ mutant neural tube; no primary cilia visible, although there are protrusions from apical surface of cells. (**M**,**N**) Sections of the mesonephric kidney (Mn) at 7 days of development stained with Haematoxylin and Eosin. (M) Wild-type embryo. (N) *talpid*$^3$ mutant embryo, note cysts (*). M, mullerian duct; G, gonad. Scales bars: 5 μm in A-F; 10 μm in G-L; 500 nm in I'; 500 μm in M,N.

cells were transfected with 0.5 μg/μl ggKIAA0586ex11/12::GFP or hsKIAA0586ex11/12::GFP, respectively, in pCAGGS using Fugene6, then observed after 5-7 hours for GFP expression, fixed in 4% PFA 10 minutes, washed three times in PBS and stored for 24 hours at 4°C, then blocked in 5%FCS/PBS+0.5% Triton for 30 minutes.

### Immunohistochemistry of cultured cells

Cells were washed in PBS, fixed in ice-cold methanol and acetone (50%) for 10 minutes, and blocked in PBS/0.2% Tween20/10% goat serum for 30 minutes.

An antibody was raised against C-terminal peptide (DSDSSGADTF) of chicken Talpid3 in rabbit. Serum from fifth bleed was used to detect overexpressed HA::ggKIAA0586 by western blot analysis, producing band of 200 kDa. Antibody was then affinity purified by coupling peptide to HiTrap NHS-activated HP column (Amersham) and tested by immunofluorescence in HEK293T cells transfected with HA::ggKIAA0586. All transfected cells were recognised by both anti-Talpid3 and anti-HA antibodies. Purified Talpid3 antibody was diluted 1:2 for cell immunofluorescence staining.

Primary antibodies used were as follows: for visualisation of primary cilia, rabbit anti-γ-tubulin 1:1000 (Sigma) and mouse anti-acetylated tubulin 1:1000 (Sigma); for actin and focal adhesions, anti-actin 1:1000 (Sigma), Alexa-Fluor-488 phalloidin 1:1000 (Molecular probes), anti-vinculin 1:1000 (Sigma); for tagged Talpid3 constructs, monoclonal mouse anti-Myc 1:1000 (Sigma) and mouse anti-Flag antibody 1:1000 (Sigma); for centrosomes, rabbit anti-pericentrin 1:5000 (abcam); for transfected cells, mouse anti-HA 1:2000 (Sigma); and for microtubules, mouse anti-α-tubulin 1:1000 (Sigma). All antibodies were applied for 1 hour at room temperature, then removed with three 5-minute washes in PBS/0.2% Tween20. Secondary antibodies were: Alexa-Fluor-488 conjugated anti-mouse 1:500 (Molecular Probes), Alexa-Fluor-546 conjugated anti-rabbit 1:500 (Molecular Probes) and Alexa-Fluor-610 conjugated anti-rabbit 1:1000 (Molecular Probes), and were incubated for 1 hour at room temperature. Samples were DAPI stained and mounted, and viewed on Zeiss LSM510 confocal microscope.

### Microtubule re-growth assay

CEFs were seeded onto cover slips in DMEM/Ham's F12 at $0.75\times10^6$/ml. 24 hours later treated with 25 μM nocodazol at 37°C for 1 hour. After nocodazol removal, cells were incubated for 0, 10 or 60 minutes, then fixed in 50% methanol/50% acetone for 10 minutes, and stained with mouse anti-α-tubulin as above.

### Cloning of the *Nematostella vectensis* Talpid3 homologue

*Nvtalpid3*, the cnidarian homologue of *Talpid3*, was cloned from *Nematostella vectensis* by extending an EST sequence using ORF predictions available for *Nematostella* genome and by RACE PCR. Primer sequences are available upon request. Putative full-length clone 6058 bp (Accession Number FJ428244) encoding conceptually translated 1708 amino acid protein, was validated by RT-PCR and sequencing.

### Bioinformatics analyses of polypeptide sequences

EMBOSS sequence analysis system (Rice et al., 2000) was used to extract amino acid sequences (SEQRET), to derive peptide statistics (PEPSTATS), to create plots of sequence conservation based on multiple sequence alignments (PLOTCON) and to produce helical wheel diagrams (PEPWHEEL) to visualise distribution of polar and non-polar residues in alpha helical regions. Multiple alignments of amino acid sequences were made using MUSCLE (Edgar, 2004) and viewed using JALVIEW (Clamp et al., 2004). PFAMSCAN (Finn et al., 2006) and PSCAN (Gattiker et al., 2002) were used to scan amino acid sequences for sequence motifs. PCOILS was used to predict coiled-coil regions (Gruber et al., 2006). Secondary structure of primary protein sequences were predicted using SABLE (Porollo et al., 2004; Wagner et al., 2005); results were displayed using POLYVIEW (Porollo et al., 2004). DOMPRO (Yoo et al., 2008), SCOOBY-DOMAIN (Pang et al., 2008) and DOMAINATION (George and Heringa, 2002) were used to predict domain boundaries, globular domains and protein domains from local gapped alignments generated using PSI-BLAST, respectively. GLOBPLOT (Linding et al., 2003) was used as described previously (Davey et al., 2006).

## RESULTS

### *talpid*$^3$ mutant chicken embryos lack primary cilia

Sections of stage HH24 wild-type chicken neural tube (Fig. 1A) and mesonephric duct (Fig. 1C) reveal well-developed ciliary axonemes projecting into the lumen (asterisk) from centrosomes (red; γ-tubulin). Cilia were also seen on limb bud mesenchyme cells (Fig. 1E); notochord cells (Fig. 1G); endothelial cells of both dorsal aorta and cardinal vein; epithelial and mesenchymal cells of somites; gut epithelia; neuroectoderm of the developing eye; endocardium; and extra-embryonic mesoderm (data not shown). By contrast, in sections of *talpid*$^3$ mutant embryos, no ciliary axonemes could be seen projecting into the lumen of the neural tube, although centrosomes were clearly visible (Fig. 1B,D); nor could primary cilia be seen on cells in the limb bud (Fig. 1F), notochord (Fig. 1H) or any of the other tissues listed above (data not shown). Scanning electron microscopy of wild-type embryos also showed that primary cilia can readily be distinguished projecting from the centre of many cells of the outer periderm layer of the limb bud ectoderm (Fig. 1I, black circles; Fig.1I′) (41/111 cells examined) and in the neural tube, projecting from pits in the apical surface of cells lining the lumen (Fig. 1K, arrows). In *talpid*$^3$ mutant embryos, no primary cilia could be seen projecting from periderm cells (Fig. 1J) (132 cells examined) nor neural tube cells (Fig. 1L).

In human ciliopathies and mouse mutants that lack primary cilia, a range of defects can occur in addition to those associated with abnormal Hh signalling, including polycystic kidneys (Bisgrove and Yost, 2006; Lehman et al., 2008). Mutant embryos from our current *talpid*$^3$ flock occasionally survive for up to 10 days, thus allowing examination of organs later in development. Histology of embryonic

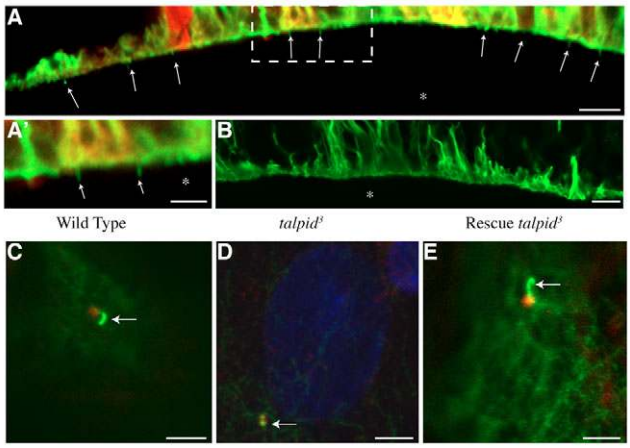


**Fig. 2. Rescue of primary cilia.** (A,B) Rescue of primary cilia in *talpid*$^3$ mutant neural tube after electroporation with construct encoding full-length chicken Talpid3. (**A**) Section of electroporated side of neural tube expressing RFP, showing rescue of primary cilia, indicated with arrows, projecting into lumen (*) and stained with acetylated tubulin (green). (**A'**) Higher magnification of outlined area in A; rescued primary cilia are indicated with arrows. (**B**) Section of non-electroporated side of neural tube, no primary cilia present. (**C-E**) Rescue of primary cilium formation in *talpid*$^3$ mutant CEFs. (C) Wild-type CEF with primary cilium axoneme stained with acetylated tubulin, (green; arrow) protruding from centrosome stained with γ-tubulin (red). (D) *talpid*$^3$ mutant CEF no primary cilia; acetylated tubulin staining (green) almost entirely overlaps with centrosome staining (red, arrow). (E) *talpid*$^3$ mutant CEF transfected with a construct encoding full-length chicken Talpid3 shows rescue of primary cilium, arrow indicates axoneme protruding from centrosome. Scale bars: 8 μm in A,B; 4 μm in A'; 3 μm in C-E.

day 7 *talpid*$^3$ mutant mesonephros (the functional embryonic kidney in chickens) revealed multiple large cysts (Fig. 1N, asterisks; compare with wild-type kidney, Fig. 1M). This is comparable with the pathology of the developing metanephric kidney seen in mice with abnormal ciliogenesis (Lehman et al., 2008).

To confirm that lack of primary cilia on *talpid*$^3$ mutant cells is a consequence of a mutation in the *Talpid3* gene (*KIAA0586*), we carried out rescue experiments in ovo by electroporating the neural tube of *talpid*$^3$ mutant embryos with a construct encoding full-length chicken Talpid3 (ggKIAA0586). We have previously shown that electroporation of this construct restored wild-type dorsoventral patterning in the neural tube of mutant embryos (Davey et al., 2006). This construct also rescued primary cilia (Fig. 2A,A′,B). Furthermore, when mutant chicken embryonic fibroblasts in culture were transfected with the same expression construct, primary cilia were rescued (Fig. 2E) ($n$=5/5 transfected cells observed, compare with Fig. 2D) and axoneme formation was comparable with that in wild-type chicken fibroblasts (Fig. 2C).

## Ultrastructural analysis of ciliogenesis and actin organisation in talpid$^3$ mutant cells

Stages in formation of a primary cilium have been deduced from detailed analysis of fibroblasts and smooth muscle cells in chicken and mammalian tissues using transmission electronmicroscopy (Sorokin, 1962; Sorokin, 1968). We therefore examined the ultrastructure of *talpid*$^3$ mutant cells to gain insights into why ciliogenesis fails.

In wild-type chicken neural tube, most cells had primary cilia projecting into the lumen (Fig. 3A,B). Each cilium emerged from a pit in the apical cell surface, and the axoneme was enclosed in a sheath of ciliary membrane and contained microtubules extending along its length (Fig. 3A,B). The basal body can be recognised by its appendages (structures including satellites and rootlets associated with the mature basal body) (Fig. 3A,B) (Sorokin, 1968). In some sections, the sister centriole located below the basal body could also be seen (Fig. 3B). By contrast, in cells of *talpid*$^3$ mutant neural tube, no primary cilia projected from apical cell surfaces into the lumen (Fig. 3C-E) (3/3 mutant embryos examined). Basal bodies (Fig. 3C-E), however, were readily identified by the presence of associated appendages (Fig. 3C-E), and these, together with their sister centrioles(s), were seen in the apical region of the cells. In some cases, a few short microtubules were present distally on the basal body (Fig. 3C) but, in most cases, no trace of axoneme development was observed. Neither were any ciliary vesicles associated with the basal bodies (Fig. 3C,D) (55/58 basal bodies observed, two embryos examined) although in three cases, a vesicle was observed nearby (Fig. 3E,E′). Therefore in *talpid*$^3$ mutant embryos, migration of the centrioles to the apical region of neural tube cells and maturation of the mother centriole into a basal body appeared unaffected, but docking, which involves fusion between the ciliary vesicle associated with the basal body and the apical cell membrane (Dawe et al., 2007; Sorokin, 1968), and subsequent axoneme

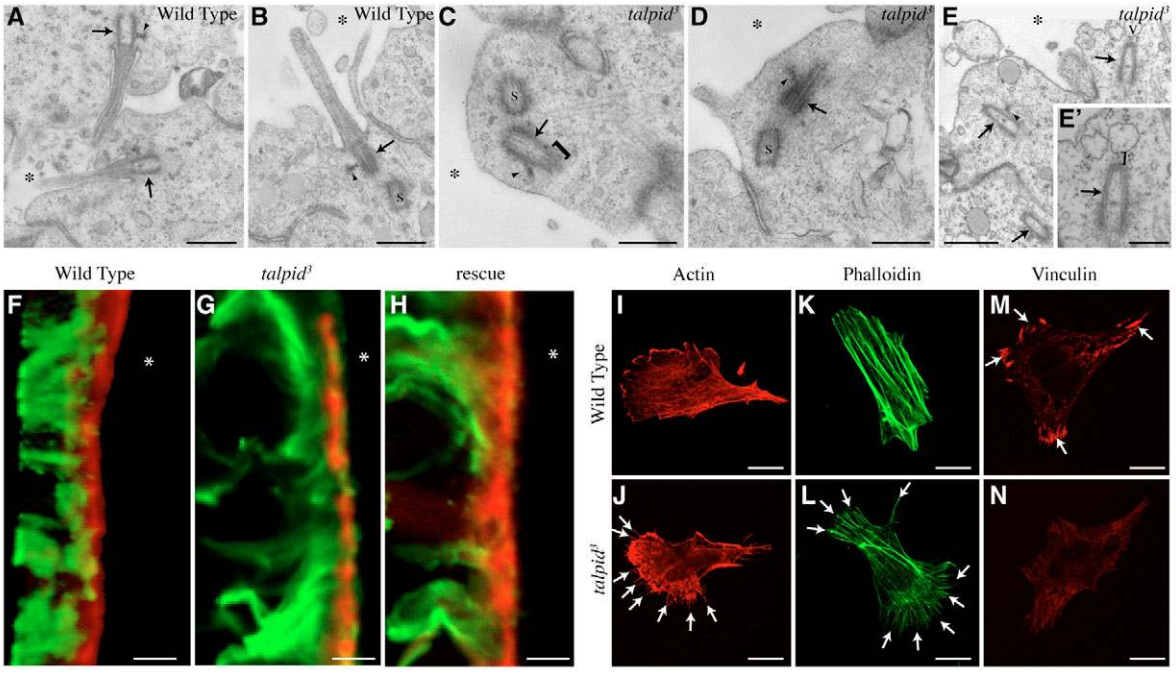


**Fig. 3. Ciliogenesis and actin organisation in wild type and *talpid*$^3$ mutant cells.** (A-E) TEM sections through neuroepithelium of stage HH24 chicken embryos. (**A**,**B**) Wild-type embryo; primary axonemes project from pits in apical cell surfaces into lumen (*); basal bodies (black arrow) with satellites (arrowhead); s, sister centrioles. (**C-E′**) *talpid*$^3$ mutant neuroepithelium. No primary cilia project from cell surface into lumen. In C, a few short microtubules are seen at distal end of basal body (bracket). In E, vesicle (v) present near basal body; (E′) Higher magnification of basal body in E showing vesicle near but not fused with basal body (bracket indicates gap). In C,D, the basal body is not orientated towards the apical surface. (**F-H**) Section showing one side of neural tube from stage HH24 embryos stained with phalloidin (red) and α-tubulin (green). (F) Wild-type embryo; an even continuous band of phalloidin staining is present at apex of cells abutting lumen (*). (G) *talpid*$^3$ mutant embryo; uneven phalloidin staining is present. (H) *talpid*$^3$ mutant embryo electroporated with a construct encoding full-length chicken Talpid3; rescue of phalloidin staining can be seen, compare with F. (**I-N**) Actin cytoskeleton of wild-type and *talpid*$^3$ mutant cells from limb buds in primary culture. Compare I with J (actin staining), and K with L (phalloidin staining). Arrows in J,L indicate actin-containing filopodia. Fewer focal adhesions expressing Vinculin (arrows in M) in *talpid*$^3$ mutant cells (N) compared with wild-type cells (M) 24 hours after seeding. Scale bars: 589 nm in A-D; 721.5 nm in E; 294 nm in E′; 11 μm in F-H; 5 μm in I-N.

formation did not occur. The TEM images of *talpid*$^3$ mutant cells also showed that basal bodies were frequently misorientated and did not lie perpendicular to the apical cell surface as in normal cells (Fig. 3C,D; see Fig. S1 in the supplementary material) [9/18 (50%) basal bodies misorientated in one *talpid*$^3$ mutant embryo; 26/40 (65%) basal bodies misorientated in another].

It has been suggested that the actin cytoskeleton in the apical region of epithelial cells orientates the basal body, allowing microtubules to polymerise into the ciliary axoneme (Park et al., 2006), and that apical actin enrichment is required for ciliogenesis (Pan et al., 2007). Confocal microscopy of transverse sections of wild-type chicken neural tube showed an even continuous band of F-actin, stained with phalloidin at the apex of cells (Fig. 3F), whereas in the *talpid*$^3$ mutant, even though there was strong staining at the cell apex, it was punctate and not continuous (Fig. 3G). Electroporation of ggKIAA0586, which rescued primary cilium formation (see Fig. 2A), also restored the continuous band of phallodin staining at the apex of *talpid*$^3$ neural tube cells on the electroporated side (Fig. 3H). Abnormalities in microfilament organisation were also seen in cultured mutant cells. *talpid*$^3$ mutant limb cells had stronger actin staining at the ruffled membrane and fewer stress fibres than did wild-type limb cells (compare Fig. 3I,K with Fig. 3J,L). In addition, there were many fine filopodia containing actin around the circumference of the mutant cells, which were not seen in wild-type cells (compare Fig. 3I,K with Fig. 3J,L), a feature previously observed in scanning electron microscopical studies on *talpid*$^3$ mutant limb bud cells in vivo (Ede et al., 1974). Discrete vinculin-positive focal adhesions were also less well defined in *talpid*$^3$ mutant limb cells than in wild-type cells (compare Fig. 3M with Fig. 3N).

## Subcellular localisation of Talpid3 protein

To verify that the Talpid3 protein is present in the centrosome [as suggested by Andersen et al. (Andersen et al., 2003)], we raised an antibody against the C terminus of chicken Talpid3 and used this in double immunofluorescence staining with γ-tubulin as a centrosomal marker in serum-starved wild-type and *talpid*$^3$ mutant chicken embryonic fibroblasts to determine the subcellular localisation of Talpid3. The *talpid*$^3$ mutation results in a premature stop codon and, even if a truncated protein was produced, this antibody would not recognise it. In wild-type fibroblasts, Talpid3 antibody staining colocalised with γ-tubulin (Fig. 4A-C), and was enriched in both centrioles (Fig. 4D-F), whereas, in *talpid*$^3$ mutant fibroblasts, Talpid3 antibody staining could not be detected in the centrosome (Fig. 4G-I).

## Cytoskeletal organisation and dynamics

The detection of Talpid3 protein in the centrosome is consistent with a role in primary cilia formation but the centrosome also directs microtubule organisation, including the mitotic spindle. We therefore examined localisation of Myc- or Flag- tagged Talpid3 during the cell cycle in HEK293T cells. Tagged Talpid3 protein (stained with antibodies against either Myc or Flag) co-localised with Pericentrin (a centrosomal marker) during interphase (Fig. 4J-L) and metaphase (Fig. 4M-O). More diffuse staining of tagged Talpid3 protein was also seen throughout the cytoplasm during anaphase (Fig. 4P-R) and telophase (Fig. 4S-U). Despite the presence of Talpid3 at the centrosome in early phases of the cell cycle, no spindle defects were observed in *talpid*$^3$ mutant cells (data not shown). In addition, there were no obvious differences in microtubule organisation between chicken embryonic fibroblasts from wild-type and *talpid*$^3$ mutant embryos (compare Fig. 5A,B with Fig. 5C,D), although there was a delay in microtubule re-growth after nocodazol treatment (compare Fig. 5E,F,I,J,M,N with Fig. 5G,H,K,L,O,P).

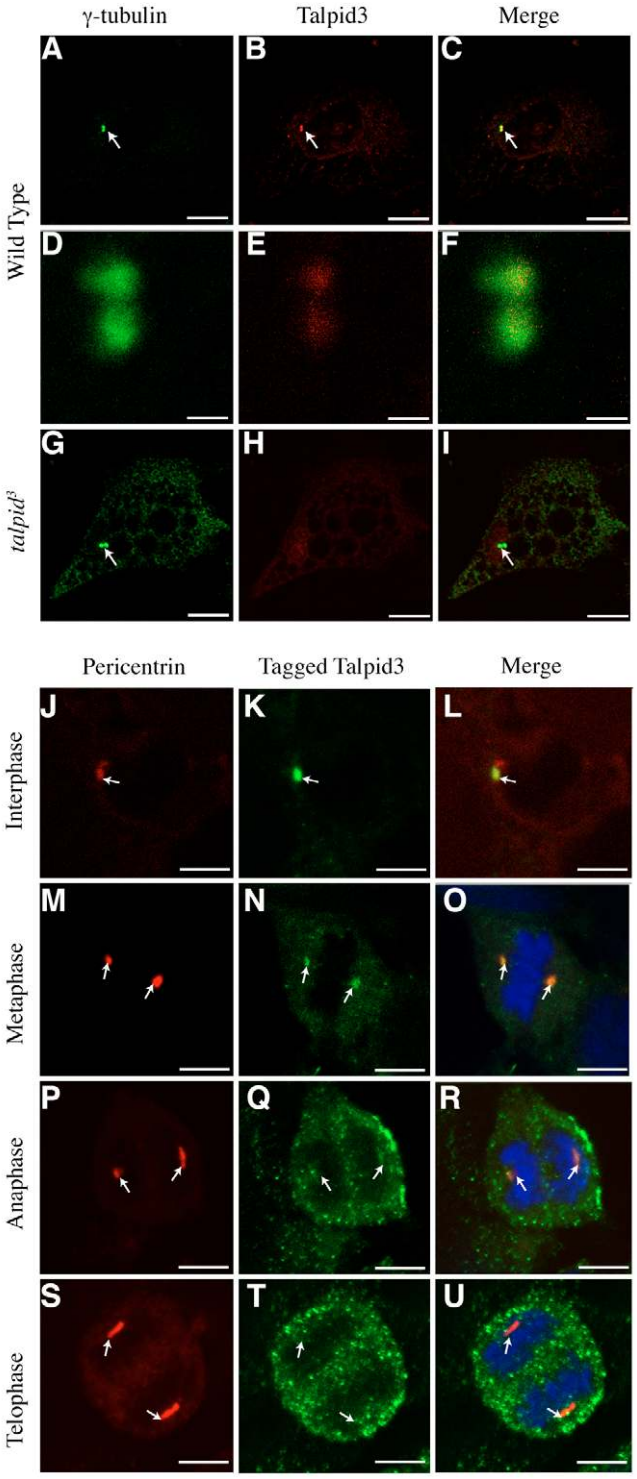


**Fig. 4. Localisation of Talpid3 protein to centrosome.** (A-I) Co-immunofluorescence staining in serum-starved CEFs; anti γ-tubulin (green) marks the centrosome; anti-Talpid3 is in red; merged images are shown in the right-hand column. (**A-C**) Localisation of Talpid3 to centrosome. (**D-F**) Higher power image of centrosome shown in A-C, Talpid3 is localised to both centrioles. (**G-I**) Talpid3 is not detected at centrosome in *talpid*$^3$ mutant cells. (**J-U**) Co-immunofluorescence staining in HEK293T cells. Pericentrin (red) marks the centrosomes (first column) (J,M,P,S); Myc (K,N) or Flag (Q,T) tagged Talpid3 protein (green) is shown in the second column; merged images are shown in third column (L,O,R,U). DNA is stained with DAPI (blue). Scale bars: 5 μm in A-C,G-I; 0.13 μm in D-F; 3 μm in J-U. Arrows indicate centrosomes.

## Bioinformatics and structure/function analysis of the Talpid3 protein

In order to identify functional domains in the Talpid3 protein, we extended our previous bioinformatics analysis (Davey et al., 2006) using orthologous cDNA sequences of *Nematostella vectensis* and a predicted homolog in the genome sequence of *Strongylocentrotus purpuratus* (Putnam et al., 2007; Sodergren et al., 2006). Alignment of vertebrate *Nematostella vectensis* and *Strongylocentrotus purpuratus* Talpid3 sequences revealed a distinct highly conserved region between amino acids 498-585 (Fig. 6A,B; see Figs S2,S3 in the supplementary material), which lies downstream of the Talpid3 mutation, which would truncate the protein at amino acid 366. This conserved region is predicted to contain a single coiled-coil domain between amino acids 498-529 (Fig. 6A,B; see Figs S2-S5 in the supplementary material) and is encoded by exons 11 and 12 (Fig. 6A).

We tested the function of this highly conserved region of the Talpid3 protein using complementation experiments in *talpid*$^3$ mutant neural tube, as before, and monitored both cilia formation and neural tube dorsoventral patterning. In *talpid*$^3$ mutant embryos, the neural tube is dorsalised and expression of ventral markers such as Nkx2.2 and Islet1 is lost, whereas expression of dorsal markers such as Pax6 and Pax7 is expanded. We have shown previously that these patterns of expression could be normalised by electroporation of constructs encoding full-length chicken Talpid3 (Davey et al., 2006). Analysis of the neural tube from *talpid*$^3$ mutant embryos electroporated with a series of constructs encoding different fragments of Talpid3 showed that the entire conserved region is essential for rescue (Fig. 7A-H). Thus, constructs containing the entire conserved region (construct D) rescued primary cilia formation (Fig. 7Q,R) and neural tube patterning (construct C, Fig. 7I-L), inducing expression of Nkx2.2 and Islet1 (Fig. 7I,J; compare RFP electroporated side with non-electroporated side) and restricting Pax6 and Pax7 expression dorsally (Fig. 7K,L). Electroporation of a construct encoding just the conserved region (Fig. 7H), however, was not able to rescue neural tube patterning. Neither primary cilia formation nor neural tube pattern was rescued by constructs encoding C-terminal fragments lacking the coiled-coil domain (construct E, Fig. 7E), the adjacent highly conserved region, amino acids 529-585 (construct F, Fig. 7F) or the entire conserved region (constructs B and G, Fig. 7B,G). Fig. 7M-P shows a *talpid*$^3$ mutant neural tube electroporated with construct E. Despite substantial RFP expression, indicating successful transfection, expression patterns of Nkx2.2, Islet1, Pax6 and Pax7 were unchanged. Thus, the conserved region is required but not sufficient to rescue dorsoventral patterning of the neural tube. It should be noted that none of the constructs (A-H) altered neural tube patterning in wild-type embryos and therefore do not show any dominant-negative effects, including construct B, which encodes the fragment of Talpid3 protein predicted to be expressed in the mutant.

To determine the function of the conserved region in centrosomal localisation, we transfected a construct encoding this region alone from the human protein (KIAA0586) fused to GFP (hsKIAA0586ex11/12::GFP) into HEK293T cells. GFP expression was seen in the centrosome (Fig. 7T) (3/3 transfected cells observed) co-localising with γ-tubulin (Fig. 7S,U). Likewise, when a construct encoding the chicken *Talpid3* conserved region fused to GFP (ggKIAA0586ex11/12::GFP) was transfected into chicken primary culture cells, co-localisation was also seen with γ-tubulin at the centrosome (data not shown). These data indicate that the conserved region is sufficient to target Talpid3 protein to the centrosome.

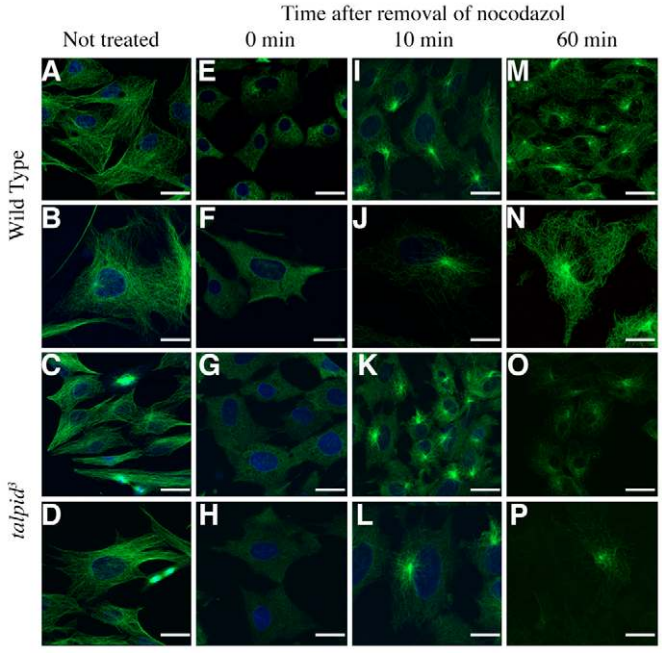


**Fig. 5. Microtubule dynamics in wild-type and *talpid*$^3$ mutant cells in culture.** Microtubule organisation visualised with anti α-tubulin (green), nuclei stained with DAPI (blue). CEFs from either wild-type (E,F,I,J,M,N) or *talpid*$^3$ mutant cells (G,H,K,L,O,P) were treated with nocodazol and microtubule regrowth assessed. (**A-D**) Untreated cells. (**E-H**) Microtubule organisation is lost when wild-type and *talpid*$^3$ cells were treated with nocodazol. (**I-L**) Ten minutes after nocodazol removal, microtubule nucleation has begun in wild-type (I,J) and *talpid*$^3$ mutant cells (K,L). (**M-P**) Sixty minutes after nocodazol removal, microtubules fully reformed in wild-type cells (M,N), but regrowth delayed in *talpid*$^3$ mutant cells (O,P). Scale bars: 20 μm in A,C,E,G,I,K,M,O; 5 μm in B,D,F,H,J,L,N,P.

## DISCUSSION

Here, we show that the *talpid*$^3$ chicken mutant lacks primary cilia and demonstrate using rescue experiments that this is a direct result of loss of Talpid3 function. Lack of primary cilia in *talpid*$^3$ chicken mutants provides an explanation for the Hh signalling defects, inability to process Gli3 (Davey et al., 2006) and similarities with mouse mutants that lack cilia and were originally highlighted as being defective in Hh signalling (Haycraft et al., 2005; Huangfu and Anderson, 2005; Huangfu et al., 2003).

Primary cilia are absent on cells in all *talpid*$^3$ chicken mutant tissues studied, including those not known to be dependent on Hh signalling, such as the mesonephric duct. A growing number of human conditions known as ciliopathies, including syndromes such as primary cilia dyskinesia, Bardet-Biedl syndrome (BBS), Joubert syndrome and Meckel syndrome (Badano et al., 2006; Bisgrove and Yost, 2006; Fliegauf et al., 2007; Tobin and Beales, 2007), have a range of defects, including those associated with abnormal Hh signalling and also polycystic kidneys. A role for primary cilia in polycystic kidney disease was first suggested after it was discovered that the genes affected in mice with polycystic kidneys, e.g. the *orpk* and *inv* mice (Lehman et al., 2008; Moyer et al., 1994; Shiba et al., 2005; Siroky and Guay-Woodford, 2006), encoded cilia associated proteins. Thus, our finding that kidneys of 7-day-old *talpid*$^3$ chicken mutant embryos are cystic is consistent with the general inability of *talpid*$^3$ mutant cells to form primary cilia. Thus, we conclude that the *talpid*$^3$ chicken mutant is a new example of a ciliopathy and a

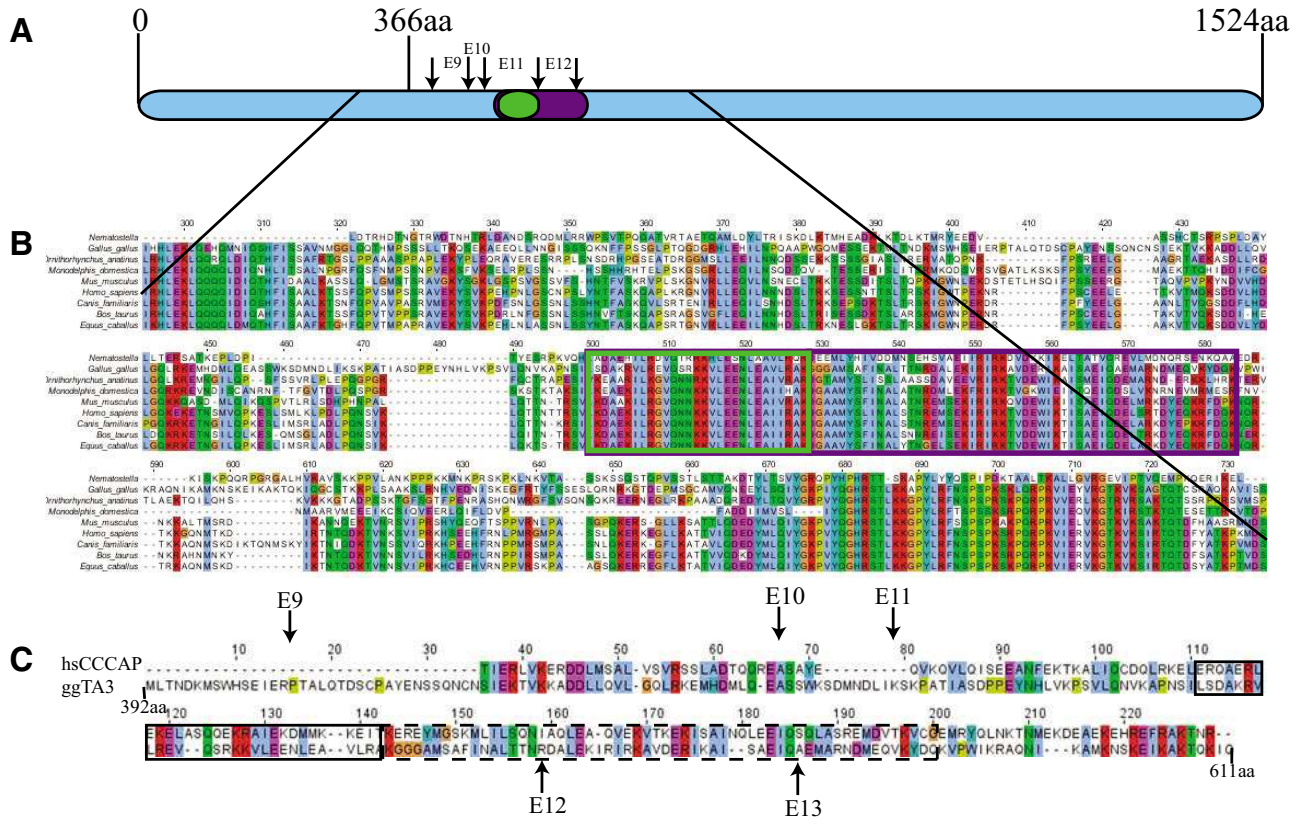


**Fig. 6. Alignment of Talpid3 proteins and domain predictions.** (**A**) Scale and location of *talpid*$^3$ mutation with highly conserved region (purple) and coiled-coil domain (green; see Fig. S4 in the supplementary material), exons 9-12 are indicated between arrows. (**B**) Multiple alignments of orthologous Talpid3 sequences (amino acids 295-735) from vertebrates and *Nematostella vectensis* using MUSCLE displayed with JALVIEW. Predicted coiled-coil region green box between amino acids 498-529; highly conserved region purple box, amino acids 498-585. Chicken sequence is used as a reference and does not contain gaps. (**C**) Distant sequence homologies between amino acids 392-611 (DOMAINATION domain 3) (see Table S1 in the supplementary material) of chicken Talpid3, and amino acids 0-229 of human CCCAP. Predicted coiled-coil region from PCOILS analysis (see Fig. S4 in the supplementary material) is shown by a solid outline; the highly conserved region is indicated by a broken outline. The locations of boundaries for domains encoded by exons 9-13 are shown by arrows.

potential model for human disease. The range of defects in different human ciliopathies varies although the reasons for this are not clear. Some ciliopathies, such as BBS, Joubert syndrome, Meckel syndrome and oral facial digital syndrome (OFD) have features that one would specifically associate with Hh signalling defects, such as polydactyly, similar to the *talpid*$^3$ mutants, whereas others, such as those caused by mutations in polycystin 1 and polycystin 2, have kidney defects. It will be interesting to define the precise spectrum of defects in *talpid*$^3$ chicken mutants for comparison with the human syndromes.

Our ultrastructural studies of cells in the *talpid*$^3$ mutant neural tube suggest that ciliogenesis fails because basal bodies do not dock at the apical cell membrane. One possible reason why docking fails in the *talpid*$^3$ mutant is that Talpid3 is involved in fusion of the ciliary vesicle to the basal body. Another centrosomal protein, BBS1, functions in this way by binding to Rabin8, a guanine nucleotide exchange factor, which activates Rab8, a Rab-GTPase that specifically traffics ciliary membrane to the base of the primary cilium (Nachury et al., 2007; Yoshimura et al., 2007). BBS1 is part of a complex of centrosomal proteins collectively termed the BBSome, which also includes BBS2, 4, 5, 7, 8 and 9. Whether the Talpid3 protein is also part of the BBSome or helps to traffic Rab8a to the cilium remains to be investigated. Another possible reason why ciliogenesis fails in the *talpid*$^3$ chicken mutant is because Talpid3 is required for apical actin enrichment. In oviduct ciliated cells, the apical actin network is closely associated with basal body appendages (Chailley et al., 1989), and recent work on *Xenopus laevis* epidermal cells with motile cilia has shown that apical enrichment of actin is required for ciliogenesis (Park et al., 2006). Therefore, it is possible that the abnormal actin organisation in *talpid*$^3$ mutant cells results in basal body misorientation, leading to failure of ciliogenesis. Apical actin enrichment is mediated by activation of RhoA (Pan et al., 2007) and it has been shown that RhoA is localised to the basal body in multiciliated cells (Park et al., 2008), thus providing an explanation for how a centrosomal protein such as Talpid3 could directly affect actin organisation. Furthermore, reduced numbers of stress fibres and focal adhesions in *talpid*$^3$ mutant cells suggests that RhoA activity is decreased (Nobes and Hall, 1999). Localisation of RhoA to the basal body in *Xenopus laevis* epidermal cells has been shown to be mediated by Inturned, an effector of the Wnt planar cell polarity signalling pathway (Park et al., 2008); interestingly, Inturned, together with Fuzzy, is required for normal cilium formation (Park et al., 2006).

We have shown that the Talpid3 protein is present in both centrioles of the centrosome. There are several mouse ciliopathy models with mutations in genes encoding centrosomal proteins,

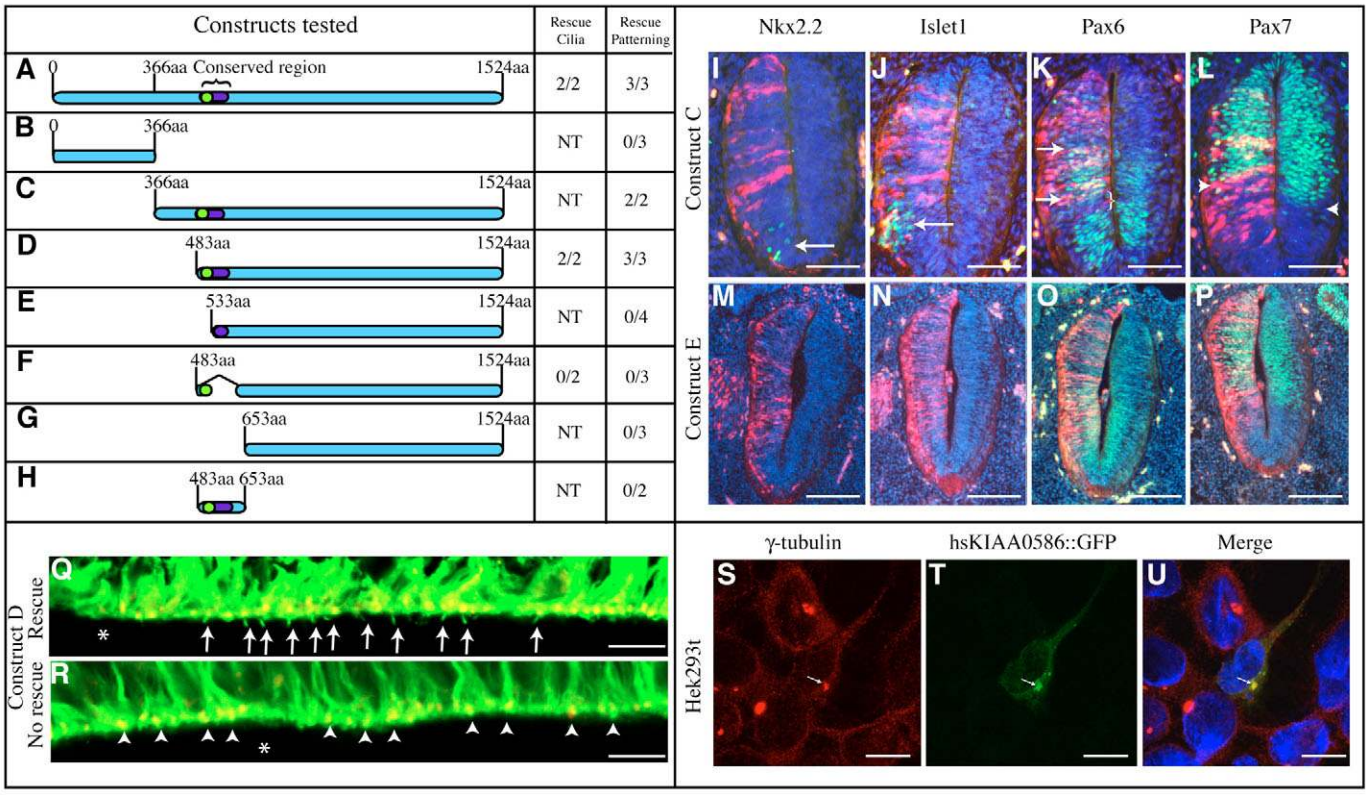


**Fig. 7. Structure/function analysis of Talpid3 protein: rescue of cilia formation and neural tube patterning in *talpid*$^{3}$ mutant embryos and centrosomal localisation.** (A-H) Schematic diagrams of chicken Talpid3 protein illustrating expression constructs used for rescue experiments. Coiled-coil domain (green) highly conserved region (purple) is shown. (**A**) Full-length Talpid3 protein. (**B**) N-terminal 1-366 amino acids, note *talpid*$^{3}$ mutation leads to premature stop codon after amino acid 366. (**C**) Amino acids 366-1524 containing highly conserved region. (**D**) Amino acids 483-1524 containing highly conserved region. (**E**) Amino acids 533-1524 lacking coiled-coil domain. (**F**) Amino acids 483-1524 containing coiled-coil domain but lacking remainder of highly conserved region. (**G**) Amino acids 653-1524 lacking highly conserved region. (**H**) Amino acids 483-653 highly conserved region only. Columns show number of *talpid*$^{3}$ mutant embryos with cilia/number of embryos tested and number of *talpid*$^{3}$ mutant embryos with neural tube patterning rescued/number of *talpid*$^{3}$ mutant embryos tested. NT, not tested. (I-P) Transverse sections of *talpid*$^{3}$ mutant neural tube electroporated with expression constructs, dorsal is upwards; ventral is downwards. Expression domains of homeodomain transcription factors (green), RFP is in red (control for transfection efficiency); nuclei stained with DAPI (blue). (I-L) Expression patterns after electroporation of construct C. (**I**) Nkx2.2 and (**J**) Islet1 (arrows) expression on electroporated side, indicated by RFP (red). (**K**) Pax6 is detected in a normal expression domain (between arrows), with a gap of non-Pax6 expressing cells indicated by white bracket. Pax6 is also expressed more ventrally where cells are not electroporated (RFP absent). (**L**) Pax7 expression is restricted more dorsally on electroporated side; compare level of arrowhead on electroporated side (RFP, red), with that on control side. (M-P) Expression patterns after electroporation with construct E, showing lack of rescue, despite successful electroporation (RFP, red). (**M**,**N**) No Nkx2.2 and Islet1 expression is induced when compared with non-electroporated side of neural tube. (**O**,**P**) Pax6 and Pax7 expression domains remain expanded ventrally on electroporated side of neural tube. (**Q**,**R**) Rescue of primary cilia in *talpid*$^{3}$ mutant neural tube following electroporation with construct D. Primary cilia are indicated with arrows, stained with anti-acetylated tubulin (green) and centrosomes indicated with arrowheads, stained with anti-γ-tubulin (red). Compare electroporated side (Q) with non-electroporated side (R). (S-U) HEK293T cells transfected with hsKIAA0586ex11/12::GFP. (**S**) γ-tubulin marks centrosome (red, arrowed). (**T**) Localisation of hsKIAA0586ex11/12::GFP fusion protein (green; arrow). (**U**) Merged image shows hsKIAA0586ex11/12::GFP colocalises with γ-tubulin in centrosome (arrow). Scale bars: 175 μm in I-P; 8 μm in Q-R; 3 μm in S-U.

including BBS1, BBS2, BBS4, OFD1 and Ftm (Davis et al., 2007; Ferrante et al., 2006; Mykytyn et al., 2004; Nishimura et al., 2004; Vierkotten et al., 2007). BBS1, BBS2, and BBS4 mutant mice still form primary cilia, although they are abnormal or degenerate, whereas both OFD1 and Ftm mutant mice lack primary cilia and have a similar phenotype to *talpid*$^{3}$ chicken mutants, including polydactyly and dorsalised neural tube. Furthermore, OFD1 has been shown to localise to both centrioles in human undifferentiated embryonic cells (Romio et al., 2004). Thus, the *talpid*$^{3}$ chicken mutant most closely resembles OFD1 mutant mice. There are no ultrastructural studies, to date, of cells from either OFD1 or Ftm mutants, and therefore it is not clear whether ciliogenesis fails at the same stage in these mutants as in *talpid*$^{3}$. Another centrosomal protein ODF2, has been suggested to be necessary for basal body docking. However, in *Odf*$^{-/-}$ cells, unlike *talpid*$^{3}$ mutant cells, basal bodies fail to mature and lack appendages (Ishikawa et al., 2005), suggesting that Talpid3 acts downstream of ODF2.

Other centrosomal proteins play roles in microtubule organisation but our observations suggest that this is not the case for Talpid3 as both the microtubule network in interphase cells and mitotic spindles appear normal in mutant cells. A change in microtubule dynamics, however, was observed in *talpid*$^{3}$ mutant cells. Ede and Flint (Ede and Flint, 1975) found that *talpid*$^{3}$ cells move slower than wild-type cells, but showed that this was not due to the *talpid*$^{3}$ mutant cells

moving intrinsically more slowly but instead spending more time at rest. This pausing might be explained by the slower rate of microtubule re-growth observed in *talpid*$^3$ mutant cells.

We have identified a region of the Talpid3 protein that is conserved all the way down to *Nematostella vectensis*. This conserved region is sufficient for centrosomal localisation and interestingly there is significant distant homology between this region in Talpid3 and a region in another centrosomal protein, CCCAP (centrosomal colon cancer autoantigen protein) (Kenedy et al., 2003) (Fig. 6C) (PSI-Blast E value 1e-47 and sequence similarity 47%). Further structure/function analysis of the Talpid3 protein showed that the highly conserved region is required but not sufficient to rescue primary cilia formation, thus suggesting that other domains in the C terminus are also required. Rescue of neural tube patterning in the mutant provides a powerful assay with which to identify these domains. A deeper understanding of the Talpid3 protein will give new insights into mechanisms involved in normal ciliogenesis and may also shed light on the basis of human ciliopathies.

This work was supported by the Biotechnology and Biological Sciences Research Council (grant numbers G20297, G20298 and BB/E014496/1). F.B. was also supported by a BBSRC Studentship, and Y.Y. and C.T. by The Royal Society. G.G. is a recipient of a Marie Curie IIF fellowship. We thank James Briscoe and Philip Beales for discussions, Lynn McTeir for technical support and the University of Bath Imaging Facility. The Islet1 and Nkx2.2 antibodies were developed by Tom Jessell. Pax6 and Pax7 antibodies were developed by Atsushi Kawakami, and were obtained from the DSHB developed under the auspices of the NICHD and maintained by the University of Iowa, Department of Biological Sciences, Iowa City, IA 52242. Deposited in PMC for release after 6 months.

**Supplementary material**

Supplementary material for this article is available at http://dev.biologists.org/cgi/content/full/136/4/655/DC1

**References**

**Andersen, J. S., Wilkinson, C. J., Mayor, T., Mortensen, P., Nigg, E. A. and Mann, M.** (2003). Proteomic characterization of the human centrosome by protein correlation profiling. *Nature* **426**, 570-574.

**Aza-Blanc, P., Lin, H. Y., Ruiz i Altaba, A. and Kornberg, T. B.** (2000). Expression of the vertebrate Gli proteins in Drosophila reveals a distribution of activator and repressor activities. *Development* **127**, 4293-4301.

**Badano, J. L., Mitsuma, N., Beales, P. L. and Katsanis, N.** (2006). The ciliopathies: an emerging class of human genetic disorders. *Annu. Rev. Genomics Hum. Genet.* **7**, 125-148.

**Bai, C. B., Auerbach, W., Lee, J. S., Stephen, D. and Joyner, A. L.** (2002). Gli2, but not Gli1, is required for initial Shh signaling and ectopic activation of the Shh pathway. *Development* **129**, 4753-4761.

**Bisgrove, B. W. and Yost, H. J.** (2006). The roles of cilia in developmental disorders and disease. *Development* **133**, 4131-4143.

**Buxton, P., Davey, M. G., Paton, I. R., Morrice, D. R., Francis-West, P. H., Burt, D. W. and Tickle, C.** (2004). Craniofacial development in the talpid3 chicken mutant. *Differentiation* **72**, 348-362.

**Caspary, T., Larkins, C. E. and Anderson, K. V.** (2007). The graded response to Sonic Hedgehog depends on cilia architecture. *Dev. Cell* **12**, 767-778.

**Chailley, B., Nicolas, G. and Laine, M. C.** (1989). Organization of actin microfilaments in the apical border of oviduct ciliated cells. *Biol. Cell* **67**, 81-90.

**Clamp, M., Cuff, J., Searle, S. M. and Barton, G. J.** (2004). The Jalview Java alignment editor. *Bioinformatics* **20**, 426-427.

**Corbit, K. C., Aanstad, P., Singla, V., Norman, A. R., Stainier, D. Y. and Reiter, J. F.** (2005). Vertebrate Smoothened functions at the primary cilium. *Nature* **437**, 1018-1021.

**Das, R. M., Van Hateren, N. J., Howell, G. R., Farrell, E. R., Bangs, F. K., Porteous, V. C., Manning, E. M., McGrew, M. J., Ohyama, K., Sacco, M. A. et al.** (2006). A robust system for RNA interference in the chicken using a modified microRNA operon. *Dev. Biol.* **294**, 554-563.

**Davey, M. G., Paton, I. R., Yin, Y., Schmidt, M., Bangs, F. K., Morrice, D. R., Smith, T. G., Buxton, P., Stamataki, D., Tanaka, M. et al.** (2006). The chicken talpid3 gene encodes a novel protein essential for Hedgehog signaling. *Genes Dev.* **20**, 1365-1377.

**Davey, M. G., James, J., Paton, I. R., Burt, D. W. and Tickle, C.** (2007). Analysis of talpid3 and wild-type chicken embryos reveals roles for Hedgehog signalling in development of the limb bud vasculature. *Dev. Biol.* **301**, 155-165.

**Davis, R. E., Swiderski, R. E., Rahmouni, K., Nishimura, D. Y., Mullins, R. F., Agassandian, K., Philp, A. R., Searby, C. C., Andrews, M. P., Thompson, S. et al.** (2007). A knockin mouse model of the Bardet-Biedl syndrome 1 M390R mutation has cilia defects, ventriculomegaly, retinopathy, and obesity. *Proc. Natl. Acad. Sci. USA* **104**, 19422-19427.

**Dawe, H. R., Farr, H. and Gull, K.** (2007). Centriole/basal body morphogenesis and migration during ciliogenesis in animal cells. *J. Cell Sci.* **120**, 7-15.

**Ede, D. A. and Flint, O. P.** (1975). Cell movement and adhesion in the developing chick wing bud: studies on cultured mesenchyme cells from normal and talpid mutant embryos. *J. Cell Sci.* **18**, 301-313.

**Ede, D. A. and Kelly, W. A.** (1964a). Developmental abnormalities in the head region of the talpid mutant of the fowl. *J. Embryol. Exp. Morphol.* **12**, 161-182.

**Ede, D. A. and Kelly, W. A.** (1964b). Developmental abnormalities in the trunk and limbs of the fowl. *J. Embryol. Exp. Morphol.* **12**, 339-356.

**Ede, D. A., Bellairs, R. and Bancroft, M.** (1974). A scanning electron microscope study of the early limb-bud in normal and talpid3 mutant chick embryos. *J. Embryol. Exp. Morphol.* **31**, 761-785.

**Edgar, R. C.** (2004). MUSCLE: multiple sequence alignment with high accuracy and high throughput. *Nucleic Acids Res.* **32**, 1792-1797.

**Eggenschwiler, J. T. and Anderson, K. V.** (2007). Cilia and developmental signaling. *Annu. Rev. Cell Dev. Biol.* **23**, 345-373.

**Eley, L., Yates, L. M. and Goodship, J. A.** (2005). Cilia and disease. *Curr. Opin. Genet. Dev.* **15**, 308-314.

**Ferrante, M. I., Zullo, A., Barra, A., Bimonte, S., Messaddeq, N., Studer, M., Dolle, P. and Franco, B.** (2006). Oral-facial-digital type I protein is required for primary cilia formation and left-right axis specification. *Nat. Genet.* **38**, 112-117.

**Finn, R. D., Mistry, J., Schuster-Bockler, B., Griffiths-Jones, S., Hollich, V., Lassmann, T., Moxon, S., Marshall, M., Khanna, A., Durbin, R. et al.** (2006). Pfam: clans, web tools and services. *Nucleic Acids Res.* **34**, D247-D251.

**Fliegauf, M., Benzing, T. and Omran, H.** (2007). When cilia go bad: cilia defects and ciliopathies. *Nat. Rev. Mol. Cell Biol.* **8**, 880-893.

**Gattiker, A., Gasteiger, E. and Bairoch, A.** (2002). ScanProsite: a reference implementation of a PROSITE scanning tool. *Appl. Bioinformatics* **1**, 107-108.

**George, R. A. and Heringa, J.** (2002). Protein domain identification and improved sequence similarity searching using PSI-BLAST. *Proteins* **48**, 672-681.

**Gruber, M., Soding, J. and Lupas, A. N.** (2006). Comparative analysis of coiled-coil prediction methods. *J. Struct. Biol.* **155**, 140-145.

**Hamburger, V. and Hamilton, H. L.** (1992). A series of normal stages in the development of the chick embryo. 1951. *Dev. Dyn.* **195**, 231-272.

**Haycraft, C. J., Banizs, B., Aydin-Son, Y., Zhang, Q., Michaud, E. J. and Yoder, B. K.** (2005). Gli2 and Gli3 localize to cilia and require the intraflagellar transport protein polaris for processing and function. *PLoS Genet.* **1**, e53.

**Huangfu, D. and Anderson, K. V.** (2005). Cilia and Hedgehog responsiveness in the mouse. *Proc. Natl. Acad. Sci. USA* **102**, 11325-11330.

**Huangfu, D., Liu, A., Rakeman, A. S., Murcia, N. S., Niswander, L. and Anderson, K. V.** (2003). Hedgehog signaling in the mouse requires intraflagellar-transport proteins. *Nature* **426**, 83-87.

**Ishikawa, H., Kubo, A., Tsukita, S. and Tsukita, S.** (2005). Odf2-deficient mother centrioles lack distal/subdistal appendages and the ability to generate primary cilia. *Nat. Cell Biol.* **7**, 517-524.

**Kenedy, A. A., Cohen, K. J., Loveys, D. A., Kato, G. J. and Dang, C. V.** (2003). Identification and characterization of the novel centrosome-associated protein CCCAP. *Gene* **303**, 35-46.

**Lehman, J. M., Michaud, E. J., Schoeb, T. R., Aydin-Son, Y., Miller, M. and Yoder, B. K.** (2008). The Oak Ridge Polycystic Kidney mouse: modeling ciliopathies of mice and men. *Dev. Dyn.* **237**, 1960-1971.

**Lewis, K. E., Drossopoulou, G., Paton, I. R., Morrice, D. R., Robertson, K. E., Burt, D. W., Ingham, P. W. and Tickle, C.** (1999). Expression of ptc and gli genes in talpid3 suggests bifurcation in Shh pathway. *Development* **126**, 2397-2407.

**Linding, R., Russell, R. B., Neduva, V. and Gibson, T. J.** (2003). GlobPlot: Exploring protein sequences for globularity and disorder. *Nucleic Acids Res.* **31**, 3701-3708.

**Marigo, V., Johnson, R. L., Vortkamp, A. and Tabin, C. J.** (1996). Sonic hedgehog differentially regulates expression of GLI and GLI3 during limb development. *Dev. Biol.* **180**, 273-283.

**May, S. R., Ashique, A. M., Karlen, M., Wang, B., Shen, Y., Zarbalis, K., Reiter, J., Ericson, J. and Peterson, A. S.** (2005). Loss of the retrograde motor for IFT disrupts localization of Smo to cilia and prevents the expression of both activator and repressor functions of Gli. *Dev. Biol.* **287**, 378-389.

**Moyer, J. H., Lee-Tischler, M. J., Kwon, H. Y., Schrick, J. J., Avner, E. D., Sweeney, W. E., Godfrey, V. L., Cacheiro, N. L., Wilkinson, J. E. and Woychik, R. P.** (1994). Candidate gene associated with a mutation causing recessive polycystic kidney disease in mice. *Science* **264**, 1329-1333.

**Mykytyn, K., Mullins, R. F., Andrews, M., Chiang, A. P., Swiderski, R. E., Yang, B., Braun, T., Casavant, T., Stone, E. M. and Sheffield, V. C.** (2004). Bardet-Biedl syndrome type 4 (BBS4)-null mice implicate Bbs4 in flagella

formation but not global cilia assembly. *Proc. Natl. Acad. Sci. USA* **101**, 8664-8669.
**Nachury, M. V., Loktev, A. V., Zhang, Q., Westlake, C. J., Peranen, J., Merdes, A., Slusarski, D. C., Scheller, R. H., Bazan, J. F., Sheffield, V. C. et al.** (2007). A core complex of BBS proteins cooperates with the GTPase Rab8 to promote ciliary membrane biogenesis. *Cell* **129**, 1201-1213.
**Nishimura, D. Y., Fath, M., Mullins, R. F., Searby, C., Andrews, M., Davis, R., Andorf, J. L., Mykytyn, K., Swiderski, R. E., Yang, B. et al.** (2004). Bbs2-null mice have neurosensory deficits, a defect in social dominance, and retinopathy associated with mislocalization of rhodopsin. *Proc. Natl. Acad. Sci. USA* **101**, 16588-16593.
**Nobes, C. D. and Hall, A.** (1999). Rho GTPases control polarity, protrusion, and adhesion during cell movement. *J. Cell Biol.* **144**, 1235-1244.
**Pan, J., You, Y., Huang, T. and Brody, S. L.** (2007). RhoA-mediated apical actin enrichment is required for ciliogenesis and promoted by Foxj1. *J. Cell Sci.* **120**, 1868-1876.
**Pang, C. N., Lin, K., Wouters, M. A., Heringa, J. and George, R. A.** (2008). Identifying foldable regions in protein sequence from the hydrophobic signal. *Nucleic Acids Res.* **36**, 578-588.
**Park, T. J., Haigo, S. L. and Wallingford, J. B.** (2006). Ciliogenesis defects in embryos lacking inturned or fuzzy function are associated with failure of planar cell polarity and Hedgehog signaling. *Nat. Genet.* **38**, 303-311.
**Park, T. J., Mitchell, B. J., Abitua, P. B., Kintner, C. and Wallingford, J. B.** (2008). Dishevelled controls apical docking and planar polarization of basal bodies in ciliated epithelial cells. *Nat. Genet.* **40**, 871-879.
**Pazour, G. J. and Rosenbaum, J. L.** (2002). Intraflagellar transport and cilia-dependent diseases. *Trends Cell Biol.* **12**, 551-555.
**Porollo, A. A., Adamczak, R. and Meller, J.** (2004). POLYVIEW: a flexible visualization tool for structural and functional annotations of proteins. *Bioinformatics* **20**, 2460-2462.
**Putnam, N. H., Srivastava, M., Hellsten, U., Dirks, B., Chapman, J., Salamov, A., Terry, A., Shapiro, H., Lindquist, E., Kapitonov, V. V. et al.** (2007). Sea anemone genome reveals ancestral eumetazoan gene repertoire and genomic organization. *Science* **317**, 86-94.
**Rice, P., Longden, I. and Bleasby, A.** (2000). EMBOSS: the European Molecular Biology Open Software Suite. *Trends Genet.* **16**, 276-277.
**Rohatgi, R., Milenkovic, L. and Scott, M. P.** (2007). Patched1 regulates hedgehog signaling at the primary cilium. *Science* **317**, 372-376.
**Romio, L., Fry, A. M., Winyard, P. J., Malcolm, S., Woolf, A. S. and Feather, S. A.** (2004). OFD1 is a centrosomal/basal body protein expressed during mesenchymal-epithelial transition in human nephrogenesis. *J. Am. Soc. Nephrol.* **15**, 2556-2568.
**Ruiz i Altaba, A.** (1999). The works of GLI and the power of hedgehog. *Nat. Cell Biol.* **1**, E147-E148.
**Shiba, D., Takamatsu, T. and Yokoyama, T.** (2005). Primary cilia of inv/inv mouse renal epithelial cells sense physiological fluid flow: bending of primary cilia and $Ca^{2+}$ influx. *Cell Struct. Funct.* **30**, 93-100.
**Siroky, B. J. and Guay-Woodford, L. M.** (2006). Renal cystic disease: the role of the primary cilium/centrosome complex in pathogenesis. *Adv. Chronic Kidney Dis.* **13**, 131-137.
**Sodergren, E., Weinstock, G. M., Davidson, E. H., Cameron, R. A., Gibbs, R. A., Angerer, R. C., Angerer, L. M., Arnone, M. I., Burgess, D. R., Burke, R. D. et al.** (2006). The genome of the sea urchin Strongylocentrotus purpuratus. *Science* **314**, 941-952.
**Sorokin, S.** (1962). Centrioles and the formation of rudimentary cilia by fibroblasts and smooth muscle cells. *J. Cell Biol.* **15**, 363-377.
**Sorokin, S. P.** (1968). Reconstructions of centriole formation and ciliogenesis in mammalian lungs. *J. Cell Sci.* **3**, 207-230.
**Tobin, J. L. and Beales, P. L.** (2007). Bardet-Biedl syndrome: beyond the cilium. *Pediatr. Nephrol.* **22**, 926-936.
**Vierkotten, J., Dildrop, R., Peters, T., Wang, B. and Ruther, U.** (2007). Ftm is a novel basal body protein of cilia involved in Shh signalling. *Development* **134**, 2569-2577.
**Wagner, M., Adamczak, R., Porollo, A. and Meller, J.** (2005). Linear regression models for solvent accessibility prediction in proteins. *J. Comput. Biol.* **12**, 355-369.
**Yoo, P. D., Sikder, A. R., Zhou, B. B. and Zomaya, A. Y.** (2008). Improved general regression network for protein domain boundary prediction. *BMC Bioinformatics* **9 Suppl. 1**, S12.
**Yoshimura, S., Egerer, J., Fuchs, E., Haas, A. K. and Barr, F. A.** (2007). Functional dissection of Rab GTPases involved in primary cilium formation. *J. Cell Biol.* **178**, 363-369.